Ti, Fe, and Ni in Si and their interactions with the vacancy and the *A* center: A theoretical study

D. J. Backlund and S. K. Estreicher*
Physics Department, Texas Tech University, Lubbock, Texas 79409-1051, USA
(Received 4 March 2010; revised manuscript received 31 March 2010; published 21 June 2010)

Transition-metal (TM) impurities from the 3*d* series have been a source of concern in Si technology for nearly 60 years. Surprisingly, numerous issues remain unresolved. In this first-principles theoretical study, we examine the properties of Ti and Ni at a similar level as that used in a recent study of Fe, except that larger supercells are used and that potential-energy surfaces are obtained using the nudged elastic band method (some Fe results have been updated). The equilibrium sites, spin and charge state(s), activation energies for diffusion, and gap levels of the isolated interstitial TMs (TM_i's) are calculated and match the measured ones when data are available. The interaction of a TM_i with a pre-existing vacancy (V) shows that the reaction $TM_i+V \rightarrow TM_s$ (substitutional TM) occurs with a large energy gain, yet smaller than the formation energy of the vacancy. The electrical properties of interstitial and substitutional TM impurities are opposite to each other. In particular, vacancies passivate or partially passivate Ti_i and Fe_i and thus may play unrecognized but beneficial roles in some processes commonly used by industry. A population analysis of the TM_s's shows that the 3*d* shell is not full, even in the case of Ni. The interaction of a TM with the *A* center ($\{O,V\}$ pair) results in two nearly energetically degenerate configurations, the $\{TM_i,O,V\}$ and the $\{TM_s,O_i\}$ complexes.

DOI: 10.1103/PhysRevB.81.235213 PACS number(s): 61.72.−y, 71.55.−i

I. INTRODUCTION

Impurities from the 3*d* transition-metal (TM) series in Si have been studied for over five decades[1,2] because they are unavoidable contaminants which reduce minority-carrier lifetimes, compromise the integrity of gate oxides, and negatively affect the performance of electronic devices. The results of the experimental and theoretical research devoted to these impurities has been reviewed several times over the years.[3–6] Today, TM impurities remain an issue in Si technology, especially for photovoltaic applications.[7–10]

The first atomic-level details about the properties of isolated 3*d* TM impurities in Si were obtained by electron paramagnetic resonance (EPR).[11–13] The TM impurities are characterized by high spins in a tetrahedral environment. Electrical measurements (see Ref. 3 for a discussion) have associated numerous gap levels to specific TM impurities. However, it was at first unclear if the electrically active levels and the EPR spectra originated from an isolated interstitial (TM_i) or substitutional (TM_s) impurity, or even some larger complex. Over the decades, a considerable number of experimental studies using magnetic, electrical, and optical techniques have uncovered various fundamental properties of isolated TMs and of some their complexes.

Early theoretical work ranged from empirical studies in clusters[14,15] to density-functional (DF) based Green's functions[16–18] methods. The impurity was assumed to be at an undistorted interstitial or substitutional site with T_d symmetry and the calculated trends were compared to the EPR or electrical measurements. Spin DF theory[19] has also been used to predict the lowest-energy spin state and gap levels of TM_s impurities. An elastic-energy approach[20] based on a hard-sphere model was used to predict the migration enthalpy of TM_i's. Finally, an approximate *ab initio* Hartree-Fock method[21] in small hydrogen-saturated clusters was used to predict the spin state, activation energy for diffusion, and binding energy to H of Ti_i and Cu_i.

Despite well over one thousand research papers, only a few properties of 3*d* TM impurities are well known. Several reviews[3–6] discuss the details and list all the references. We only mention here the key features of 3*d* TM impurities. References to specific data will be given in the text when discussing our predictions in the context of earlier experimental or theoretical studies.

(1) Isolated 3*d* TM impurities in Si are stable at the tetrahedral interstitial (T) site, with the highest spin compatible with the charge state of the impurity. (2) The activation energy for diffusion is largest for the lightest and smallest for the heaviest element of the series. It ranges from 1.79 eV for Ti_i (Ref. 22) to 0.69 eV for Fe_i (Ref. 5) to 0.18 eV for Cu_i.[23] The latter is the fastest-diffusing impurity in Si.

(3) The high-temperature solubility is smallest for the lightest and largest for the heaviest element of the series.[3] The TM impurities, introduced at high temperatures, are always far above their solubility limit at room temperature. As a result, the fast-diffusing 3*d* TMs tend to find traps (such as the $\{Fe_iB_s\}$ pair[5] or the Cu_0 defect[24]), form clusters, precipitate at surfaces, at grain boundaries or other defects, form silicides, etc. The slowest diffusers Ti and V remain isolated.

(4) The electrical activity of isolated 3*d* TM_i's decreases from the lightest to the heaviest element. Ti_i has double donor, donor, and acceptor levels[25,26] in the gap, Fe_i has only one deep donor level,[5] and isolated Ni_i has no known gap level.

(5) The 3*d* TM_i's strongly interact with radiation damage.[27–33] Several new deep-level transient spectroscopy (DLTS) lines have been reported following irradiation, but the structure of the associated defects is unknown or tentative. In Czochralski-grown Si, irradiation commonly produces $\{O,V\}$ pairs (*A* centers) whose annealing behavior is strongly affected by the presence of TM impurities in the sample.

(6) The 3*d* TMs also interact with hydrogen.[34–38] Many (but not all) of the resulting complexes are electrically active. The structures of the $\{TM,H_n\}$ complexes have not been identified experimentally, but theoretical studies are under way.

In this paper, we present the results of systematic first-principles calculations of Ti_i, Fe_i, and Ni_i, their interactions with the vacancy and the *A* center, and the properties of Ti_s, Fe_s, and Ni_s. Most of the new results are for Ti and Ni, but we also include comparisons to our recent calculations for Fe (Refs. 39 and 40) (the key results have been updated to the present level of theory). A few comparisons to Cu (Refs. 41–43) are also given. In addition to the equilibrium structures, we calculate the activation energies for diffusion, binding energies, and approximate donor and acceptor levels.

The key results can be summarized as follows. First, we use the nudged-elastic band (NEB) method to predict the minimum-energy path and activation energies for interstitial TM diffusion, the trapping of interstitial TM's by vacancies, and the transition between two TM-O*V* pair configurations. Second, we predict that the activation energy for diffusion of Ni is less than half the most commonly used experimental value. Third, we predict that vacancies, which are often generated during the processing of solar cells, play an unrecognized role in improving minority carrier lifetimes by passivating some of the most feared TM_s's. Vacancy passivation has not been reported to date. However, we confirm that Ni_i is electrically activated by vacancies as it becomes Ni_s. Fourth, we discuss the details of TM interactions with the *A* center.

Section II describes the level of theory. Sections III–VI deal with the properties of isolated TM_i's, TM_i-vacancy interactions, the properties of isolated TM_s's, and TM_i interactions with the *A* center, respectively. The key results are discussed in Sec. VII.

II. METHODOLOGY

Our first-principles electronic structure and *ab initio* molecular-dynamics simulations[44] are based on the SIESTA method.[45,46] The host crystal is represented by periodic supercells containing 216 host atoms. The lattice constant of the perfect cell is optimized in each charge state. The defect geometries are obtained with a conjugate gradient algorithm. A $3\times3\times3$ Monkhorst-Pack[47] mesh is used to sample the Brillouin zone for the calculation of gap levels, which is done using the marker method.[48,49] Our implementation of this method uses the perfect crystal as the universal marker for all the defects, thus eliminating the dependence of the predictions on the marker. The potential-energy surfaces are mapped using the NEB method.[50,51] The NEB calculations are done in a 64 host-atoms cell and a $2\times2\times2$ mesh.

The electronic core regions are removed from the calculations using *ab initio* norm-conserving pseudopotentials with the Troullier-Martins parameterization[52] in the Kleinman-Bylander form.[53] The SIESTA pseudopotentials have been optimized using the experimental bulk properties of the perfect solids and/or first-principles calculations[54] as well as vibrational properties of free molecules or known defects, when such experimental data are available. Such testing leads to some fine tuning of the pseudopotential parameters relative to the purely atomic ones: small changes in the core radii and/or use of semicore states. Once optimized, we take these pseudopotentials to be transferable to the defect problems at hand. Pruneda *et al.*[55] have studied Fe/Si systems and shown that the pseudopotential/SIESTA approach provides results in excellent agreement with the all-electron tight-binding linear muffin-tin orbital method.

The valence regions are treated with first-principles spin-density-functional theory within the generalized gradient approximation for the exchange-correlation potential.[56] The basis sets for the valence states are linear combinations of numerical atomic orbital:[57] a double-zeta basis set (two sets of valences *s* and *p*'s) for O plus polarizations functions (one set of *d*'s) for Si. The basis set for the TMs consists of two sets of valences *s* and *d*'s and one set of *p*'s (semicore, in the case of Ni). The charge density is projected on a real-space grid with an equivalent cutoff of 350 Ry to calculate the exchange-correlation and Hartree potentials.

We have compared the accuracy of SIESTA (pseudoatomic basis sets) to the plane-wave VASP approach for Fe-related defects in Si and found only very small differences.[39,40] The accuracy of SIESTA is well documented in many defect problems, such as the calculations of the temperature dependence of very short and very long vibrational lifetimes.[58]

III. ISOLATED TM_i'S

The isolated Ti_i, Fe_i, and Ni_i impurities are stable at the T site with only small breathing-mode relaxations of the Si nearest neighbors (NNs). For example, in the 0 charge state, the distance between the TM_i and these four Si atoms is 2.521 Å for Ti, 2.422 Å for Fe, and 2.438 Å for Ni (the unrelaxed distance is 2.367 Å).

Note that in most charge and spin states, Ti_i and Fe_i are orbital doublets or triplets and therefore Jahn-Teller unstable. However, the EPR data[11–13] do show tetrahedral symmetry suggesting that the Jahn-Teller distortion is very small or is dynamic, in which case the symmetry is tetrahedral on the average. The proper description of static Jahn-Teller systems should involve vibronic states which are incompatible with the Born-Oppenheimer approximation implied in all first-principles studies.

In the neutral charge state, the *atomic* orbital populations are $3d^2 4s^2$ (Ti), $3d^6 4s^2$ (Fe), and $3d^8 4s^2$ (Ni). At the T site, these populations are $3d^{2.8} 4s^{0.7}$ (Ti_i), $3d^{6.5} 4s^{0.7}$ (Fe_i), and $3d^{8.5} 4s^{0.7}$ (Ni_i). In each case, the $4s$ population decreases as the $3d$ population increases. The TM_i's weakly (but covalently) overlap with each Si NNs and second NNs. The overlap populations are small but positive: 0.18 and 0.14 for Ti_i; 0.16 and 0.13 for Fe_i; and 0.10 and 0.06 for Ni_i. Thus, the usual assumption that an isolated $3d$ TM_i behaves like the atomic species is only approximately correct.

Comparisons of the measured (solid lines) and calculated (dashed lines) donor and acceptor levels are shown in Fig. 1. The measured and the calculated values are compared in Table I.

The stable spin states for each possible charge state match the measured values[11–13,59–61] and the ones calculated by other authors.[18,19] Ti_i has spin 1, 3/2, 1, and 3/2 in the ++, +, 0, and − charge states, respectively. The other *a priori* possible spin states are more than 0.5 eV higher in energy. Fe_i has spin 3/2 and 1 in the + and 0 charge states,

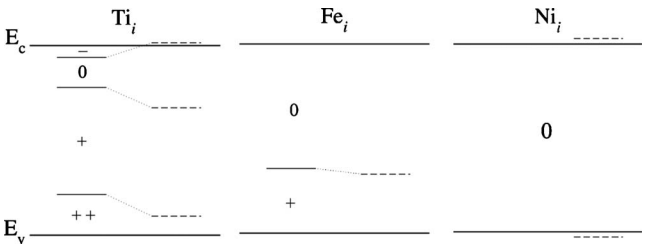

FIG. 1. Measured (solid lines) and calculated (dashed lines) donor and acceptor levels for Ti_i, Fe_i, and Ni_i. We find donor and acceptor levels of Ni_i to be in valence and conduction bands, respectively. The charge state of each impurity for various positions of the Fermi level are indicated. The references for the measured values are in Table I.

respectively;[40] Ni_i is always in the 0 charge state with spin 0. The spin 1 state is about 1 eV higher in energy.

The diffusion path is a straight T-T line with the saddle point at the hexagonal interstitial site. The calculated (measured) activation energies for diffusion in electron volt are 1.79, 1.66, 1.75, and 1.66 for Ti_i^{++}, Ti_i^{+}, Ti_i^{0}, and Ti_i^{-}, respectively (1.79 at high temperatures[22]); 0.69 and 0.76 for Fe_i^{+} and Fe_i^{0}, respectively (0.69 and 0.84, respectively[5]); and 0.21 for Ni_i^{0}. The most commonly cited experimental value for the activation for diffusion of Ni_i is 0.47.[62] However, the diffusivity of Ni_i is difficult to measure. The published prefactors D_0 range from 10^{-13} to 10^{3} cm^2/s and the activation energies from 0.13 to 4.24 eV (for a review, see Ref. 63). In the case of Cu_i^{+}, the NEB method predicts an activation energy for diffusion of 0.18 eV, which matches the most recent experimental value.[23] Note that our earlier value[21] of 0.24 eV was obtained from *ab initio* Hartree-Fock calculations in small hydrogen-saturated clusters.

IV. TRAPPING AT PRE-EXISTING VACANCIES

The $3d$ TM_i's strongly interact with radiation damage.[27–33] In this section, we consider the interactions between a TM_i and a pre-existing vacancy (V). Vacancies are generated during irradiation and implantation, as well as during various high-temperature processes such as those associated with the formation of some surface layers in PV manufacturing, such as SiN_x antireflection coatings or Al back contacts. During such nonequilibrium processes, large concentrations of charge carriers are often present. We therefore assume that the Fermi level is midgap. The interacting species are then in the 0 charge state, except for Ti_i which is in the + charge state. Closer to an equilibrium situation, it is unlikely that Ti_i^{+}, Ti_i^{++}, or Fe_i^{+} would interact with V^{++}, the stable charge state[64] in p-Si. Minority carriers would need to be produced for such interactions to take place. We assume here that all the interactions take place during the nonequilibrium phase.

TABLE I. Calculated (measured) gap levels of Ti_i, Refs. 25 and 26, Fe_i, Ref. 5, and Ni_i (no gap levels for isolated Ni_i are reported in the literature). The donor (acceptor) levels (in eV) are given relative to the valence (conduction) band as E_v+x (E_c-x).

Level	Ti_i	Fe_i	Ni_i
(0/–)	–(0.09)		
(+/0)	0.76 (0.89)	0.37 (0.39–0.45)	
(++/+)	0.15 (0.25)		

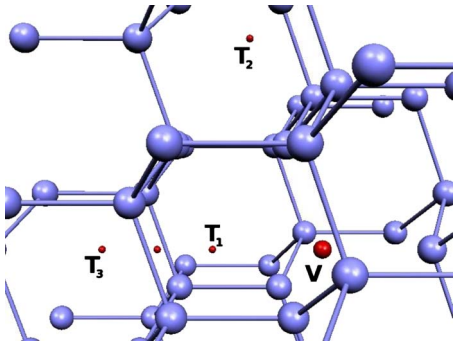

FIG. 2. (Color online) The first-, second-, and third-nearest T sites to the vacancy (red dot) are labeled T_1, T_2, and T_3, respectively. The hexagonal interstitial site is halfway between T_1 and T_3.

Thus, our initial configuration has the TM_i at the third-nearest T site to the vacancy in the spin and charge states consistent with the Fermi energy near midgap: $^{3/2}Ti^{+}$, $^{1}Fe^{0}$, and $^{0}Ni^{0}$. The final configuration for the NEB calculation has the TM at the substitutional site in the same spin and charge state. The TM moves along the trigonal axis $T_3 \rightarrow$ hexagonal $\rightarrow T_1 \rightarrow V$ (the various sites are shown in Fig. 2). Once the TM is at the substitutional site, the electronic spin flips to the lowest-energy state ($^{1/2}Ti^{+}$, $^{0}Fe^{0}$, and $^{0}Ni^{0}$) at an additional gain in energy in the case of Ti_s and Fe_s. The results are shown in Fig. 3. Note that if the TM_i starts at T_2, the second-nearest T site to the vacancy, constant-temperature molecular-dynamics simulations show that the vacancy first moves toward the TM_i which then finds itself at a site equivalent to T_1.

The energy gains in the $TM_i+V \rightarrow TM_s$ reaction (lowest-energy spin state in both configurations) using the NEB method in the Si_{64} cell ($2\times2\times2$ mesh) and using total-energy differences in the Si_{216} cell ($3\times3\times3$ mesh) are very similar: 2.07 eV and 2.02 eV for Ti^{+}, 3.20 eV and 2.93 eV for Fe, and 2.68 eV and 2.60 eV for Ni, respectively.

Note that the potential-energy surface in Ref. 39 was not obtained with the NEB method. Instead, a constant force was imposed and it pushed Fe from the interstitial to the substitutional site along the trigonal axis. The result was a more pronounced minimum outside the vacancy than obtained here. This local minimum became shallower as the magnitude of the applied force was reduced. The potential surfaces shown in Fig. 3 show that, if the TM_i starts at the T_3 site, it becomes TM_s in all cases.

The binding energies E_b (eV) of TM_i to the vacancy, defined from the reaction $TM_i+V \rightarrow TM_s+E_b$ (all in the 0 charge state), are shown in Fig. 4. They are all on the order of 3 eV, which is a substantial energy gain but is less than the formation energy of the vacancy, 3.96 eV at the present of theory. Even in the most favorable case, Fe, none of the TM_i's becomes substitutional unless a vacancy is provided by some energetic process. Note that the general shape of the

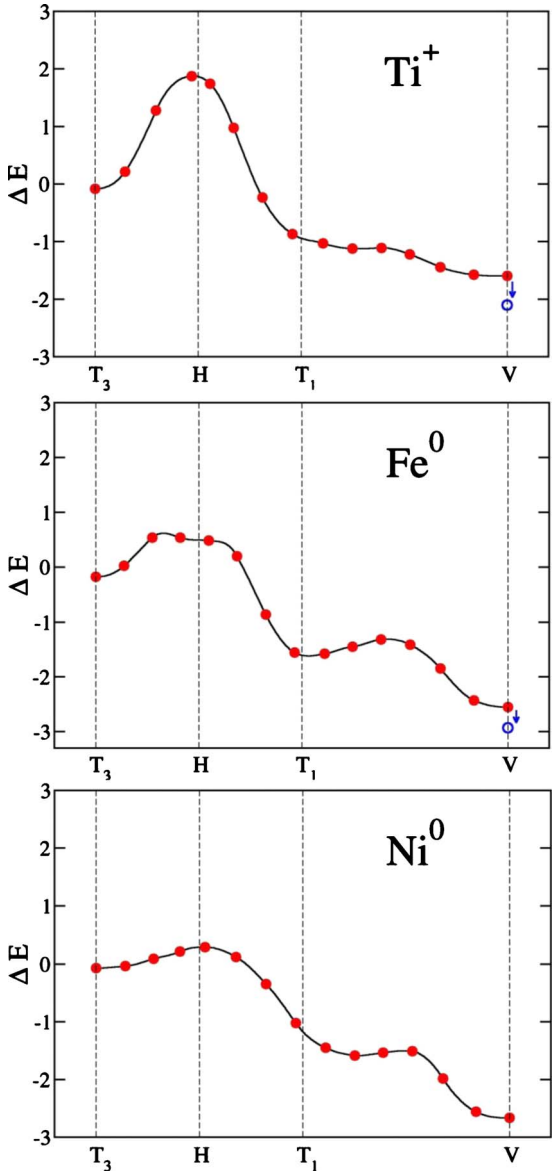

FIG. 3. (Color online) Calculated potential-energy surface for the reaction $TM_i+V \rightarrow TM_s$ in the 0 charge state along a $T_3 \rightarrow$hexagonal$\rightarrow T_1 \rightarrow V$ path with the TM_i starting at T_3 and ending at the substitutional site. The zero of the energy corresponds to the TM_i infinitely far away from the vacancy. The energy of a TM_i at the T_3 site is almost the same as at an isolated T site. The charge and spin states are fixed during the NEB calculation and corresponds to that of the isolated interstitial with Fermi energy at midgap: $^{3/2}Ti^+$, $^1Fe^0$, and $^0Ni^0$. At the substitutional site, the lowest-energy spin states are $^{1/2}Ti^+$, $^0Fe^0$, and $^0Ni^0$. The energy gain associated with the spin flip is shown with a blue arrow and open circle. Ni remains in the spin 0 state throughout the reaction.

curve in Fig. 4 is very similar to a prediction by Pauling[65] about the number of unpaired electrons along the 3*d* TM series, interpreted here as the number of electrons available for covalent bonding.

V. VACANCY PASSIVATION AND VACANCY ACTIVATION

Substitutional TM impurities are on-site with very little distortion or breathing-mode relaxation. In the 0 charge state,

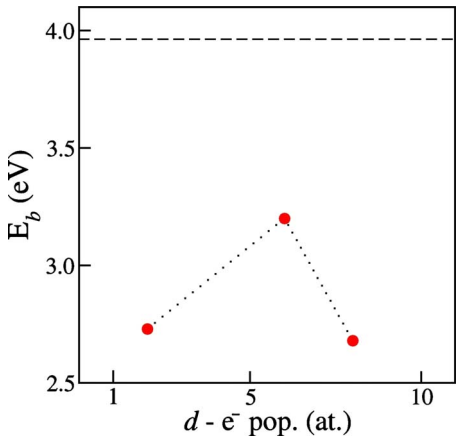

FIG. 4. (Color online) Binding energies E_b (eV) for the reaction $TM_i+V \rightarrow TM_s+E_b$, all in the 0 charge state, plotted as a function of the number of *d* electrons in the atomic species (Ref. 65). The horizontal dashed line shows the formation energy of the vacancy, 3.96 eV at the present level of theory.

the distance between the TM_s and its four Si NNs is 2.519 Å for Ti; 2.247 Å for Fe; and 2.281 Å for Ni (the unrelaxed distance is 2.367 Å).

The measured (solid lines) and the calculated (dashed lines) donor and acceptor levels are shown in Fig. 5. We are not aware of any experimental data for Ti_s. The acceptor level of Fe has been only "tentatively attributed to an acceptor state of Fe_s."[27] The measured and the calculated values are compared in Table II.

A comparison of Figs. 1 and 5 shows that the electrical properties of TM_i and TM_s defects are opposite to each other. Ti_i, with few 3*d* electrons, is a major trap for minority carriers in *p*-Si, but Ti_s is almost electrically inactive as its odd electrons pair up with those in the Si dangling bonds in order to form Ti-Si bonds. Fe_i has a deep donor level and is a strong recombination center in *p*-Si, but Fe_s has a deep acceptor level instead and is in the 0 charge state in *p*-Si, rendering it almost harmless. Thus, vacancies partially passivate some of the most feared interstitial 3*d* TMs.

On the other hand, isolated Ni_i is always in the 0 charge state while Ni_s has multiple levels in the gap. However, Ni_i is a fast diffuser which rapidly forms electrically active precipitates or silicides.[4,67,68] Our results indicate that the interaction of a single Ni with a vacancy already produces an electrically active center.

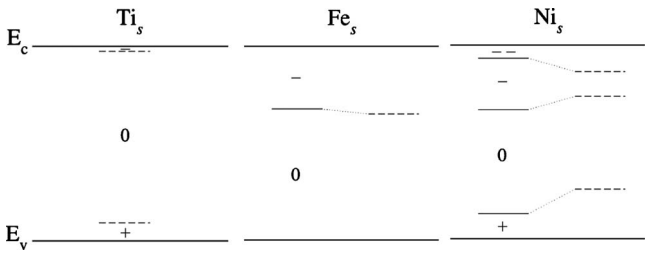

FIG. 5. Measured (solid line) and calculated (dashed lines) donor and acceptor levels of Ti_s, Fe_s, and Ni_s. The predicted charge state of each impurity for various positions of the Fermi level is indicated. The references for the measured values are in Table II.

TABLE II. Calculated (measured) gap levels of Ti_s (no gap levels for Ti_s are reported in the literature), Fe_s (Ref. 27) (see text), and Ni_s (Refs. 4, 35, and 66). The donor (acceptor) levels (in eV) are given relative to the valence (conduction) band as E_v+x (E_c-x).

Level	Ti_s	Fe_s	Ni_s
(−/−−)			0.16 (0.08)
(0/−)	0.03(−)	0.41 (0.38)	0.31 (0.39–0.47)
(+/0)	0.11(−)		0.30 (0.15–0.18)

Our stable spin states match the ones calculated by other authors.[19] Ti_s has spin 1/2, 0, and 1/2 in the +, 0, and − charge states. The other *a priori* possible spin states are at least 0.5 eV higher in energy. Fe_s has spin 0 and 1/2 in the 0 and − charge states, respectively.[39] Ni_s has spin 1/2, 1, 3/2, and 1 in the +, 0, −, and −− charge states, respectively. The spin 1/2 state of Ni_s^- is only 0.14 eV higher in energy.

Ti and Fe are partially passivated by the vacancy because their odd electrons pair up with those in the Si dangling bonds resulting in covalent overlap (energy gain) and low spin. On the other hand, Ni must open its (initially closed) $3d$ shell (energy cost) in order to achieve covalent overlap with its four Si NNs (energy gain). The open shell results in electrical activity and high spin. This is the likely reason why Ni precipitates are electrically active.

The orbital populations are $3d^{2.4}4s^{1.0}$ (Ti_s), $3d^{6.5}4s^{1.0}$ (Fe_s), and $3d^{8.4}4s^{1.0}$ (Ni_s). The overlap populations between the TM_s and each of its four Si NNs are 0.31 for Ti_s, 0.34 for Fe_s, and 0.21 for Ni_s. These covalent overlaps are much larger than for the TM_i's and show that the electrons promoted from the $3d$ shell to the $4sp$ shell hybridize with the Si dangling bonds, even in the case of Ni. The formation of these four TM_s-Si bonds is responsible for the energy gain E_b in the reaction $TM_i+V \rightarrow TM_s+E_b$.

An explanation for the EPR and electron-nuclear double resonance (ENDOR) data[69–72] of the late (atomic nd^9 or nd^{10}, $n=3$, 4, 5) substitutional TM impurities was proposed by Watkins and Williams.[73] The assumptions are that the nd shell lies deep in the valence band and is therefore always full (nd^{10}), and that the electrical activity of these TM_s's is due to the t_2-like orbitals of the four Si NNs to the vacancy. Thus, the TM_s only perturbs the vacancy states. Ammerlaan and van Oosten[74] proposed instead a model which involves a $3d^9$ configuration and sp hybridization involving the TMs and two of the four Si dangling bonds. Such a configuration has C_{2v} symmetry before any Jahn-Teller distortion. This is a variation in the Ludwig-Woodbury[13] model which involves hybridization between the TMs and all four Si dangling bonds. Here, the symmetry is T_d before any Jahn-Teller distortions.

Our population analysis supports the latter model, but it is no proof of it, for two reasons. First, our atomiclike basis set does not describe true electronic states. Within density-functional theory, only the total density obtained from a self-consistent solution of the Kohn-Sham equation represents the true electron density. The single-particle states correspond to effective particles which resemble—but are not—electrons.

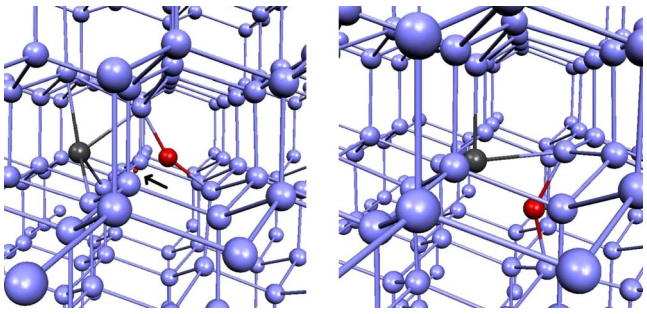

FIG. 6. (Color online) The $\{TM_i,O,V\}$ (left) and $\{TM_s,O_i\}$ (right) complexes are two nearly energetically degenerate configurations resulting from the interaction of a TM_i (dark sphere) with the $\{OV\}$ pair. In $\{TM_i,O,V\}$, the TM_i traps near the T site adjacent to a Si displaced from its substitutional site. The O atom (red sphere) overlaps with Ti_i but not Fe_i or Ni_i. The arrow points toward the vacancy site (red dot). In $\{TM_s,O_i\}$, the TM expels the O from the vacancy and takes its place. The O atom is at a puckered bond-centered site.

When comparing *ab initio* Hartree-Fock orbital and density-functional orbitals populations, one obtains similar, but not identical, numbers. Second, the Born-Oppenheimer approximation is incompatible with vibronic coupling.

VI. INTERACTIONS WITH THE *A* CENTER

The irradiation of Czochralski Si generates the *A* center ($\{O,V\}$ pair). This results from the trapping of a vacancy by an O interstitial.[75] The *A* center has an acceptor level at $E_c-0.17$ eV, begins to anneal out at 300 °C, and disappears at 375 °C. Our calculations give $O_i+V \rightarrow \{O,V\}+2.13$ eV. We find that the isolated *A* center has an acceptor level at $E_c-0.15$ eV, very close to the measured one.

When Fe, Ni, or Cu are present in the sample, the *A* center begins to anneal below 200 °C and disappears at 275 °C. A new DLTS line correlates with the disappearance of the *A* center and is associated with a $\{TM,O,V\}$ complex. In the case of Fe,[28,76,77] it is an acceptor level at $E_c-0.36$ eV, which matches the one predicted in Ref. 39 for the $\{Fe_s,O_i\}$ defect. In the case of Ni,[30,31] a new donor level at $E_c-0.365$ eV has been associated with a $\{Ni_i,O,V\}$ defect with Ni_i near but outside $\{O,V\}$. The latter structure, predicted by semiempirical Hartree-Fock calculations, has not been considered in our earlier Fe work.[39] We have now examined the $\{TM_i,O,V\}$ and $\{TM_s,O_i\}$ structures (Fig. 6), calculated their binding energies, and mapped the potential barrier between them using the NEB method.

The $\{TM_i,O,V\}$ configuration[30,31] has an interstitial TM trapped near the most favorable T site adjacent to the *A* center. The stability of this structure relative to the isolated TM_i and *A* center comes from the increased covalent overlap between the TM and a Si atom displaced by O from its ideal substitutional site. Ti_i overlaps with four Si atoms (overlap populations 0.28, 0.16, 0.14, and 0.14, respectively) and exhibits some overlap with O (0.14) and three other Si atoms (0.09, 0.06, and 0.05, respectively); Fe_i overlaps with seven Si atoms (overlap populations 0.26, 0.25, 0.25, 0.19, 0.14,

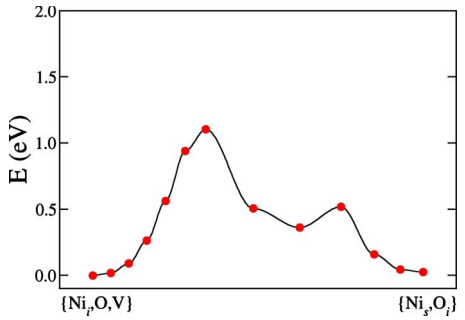

FIG. 7. (Color online) Minimum-energy path between $\{Ni_i,O,V\}$ and $\{Ni_s,O_i\}$ calculated with the NEB method in the 0 charge state. The barriers are slightly higher in the case of Fe and Ti.

0.14, and 0.10, respectively); Ni_i overlaps with two Si atoms (overlap populations 0.19 and 0.16, respectively) and weakly overlaps with four other Si atoms (0.09, 0.07, 0.03, and 0.03, respectively). In all cases, the TM_i takes advantage of the lattice distortion near the *A* center to increase its overlap with more Si neighbors. In the 0 charge state, the reaction $TM_i+\{OV\}\rightarrow\{TM_i,O,V\}$ leads to energy gains of 1.54, 1.19, and 1.21 eV in the case of Ti, Fe, and Ni, respectively.

The $\{TM_s,O_i\}$ configuration involves the transformation of TM_i plus the $\{O,V\}$ pair into TM_s with an adjacent O_i. Its stability comes from the energy gained from the $TM_i\rightarrow TM_s$ reaction (about 3 eV as discussed above) minus the energy cost associated with displacing O from the *A*-center configuration to the interstitial one (about 2 eV in our calculations). In the 0 charge state, the reaction $TM_i+\{O,V\}\rightarrow\{TM_s,O_i\}$ leads to energy gains of 1.31, 1.19, and 1.21 eV in the case of Ti, Fe, and Ni, respectively.

Figure 7 shows the potential-energy barrier separating the $\{TM_i,O,V\}$ and $\{TM_s,O_i\}$ configurations. The high barrier, associated with the changes in the Si-O bonding, makes it likely that both configurations coexist. Note that $\{TM_i,O,V\}$ is favored for Ti but the two configurations are degenerate in the case of Fe and Ni.

The calculated gap levels of the $\{TM_i,O,V\}$ complexes are as follows. $\{Ti_i,O,V\}$ has double donor and donor levels at $E_v+0.11$ eV and $E_v+0.17$ eV, respectively; $\{Fe_i,O,V\}$ has only an acceptor level at $E_c-0.38$ eV, and $\{Ni_i,O,V\}$ has a shallow acceptor level at $E_c-0.06$ eV. The only good match with a measured value is for the acceptor level of $\{Fe_i,O,V\}$: $E_c-0.38$ eV, close to the measured $E_c-0.36$ eV.[28]

The calculated gap levels of the $\{TM_s,O,V\}$ complexes are as follows. $\{Ti_s,O_i\}$ has a shallow donor level at $E_v+0.07$ eV, as well as acceptor and double acceptor levels at $E_c-0.29$ eV and $E_c-0.09$ eV, respectively; $\{Fe_s,O_i\}$ has a donor level at $E_v+0.08$ eV and an acceptor level at $E_c-0.22$ eV. Finally, $\{Ni_s,O_i\}$ has shallow donor and an acceptor levels at $E_v+0.04$ eV and $E_c-0.19$ eV, respectively. The levels shallower than $\sim$0.1 eV are not reliable because the associated wave function can easily extend beyond the volume of the supercell, and therefore be artificially confined.

The energy level at $E_c-0.365$ eV observed[31] in irradiated Ni-doped samples does not fit any of the calculated levels associated with the $\{Ni_i,O,V\}$ or $\{Ni_s,O_i\}$ complexes. However, it is close to the acceptor level of Ni_s (Table II), a defect which occurs in irradiated samples.

The acceptor level of $\{Fe_s,O_i\}$ at $E_c-0.22$ eV was found[40] to be at $E_c-0.36$ eV in the smaller 64 host-atoms supercell. The 0.14 eV difference could be attributed to two factors. First, the larger Madelung energy correction in the smaller cell. Second, we calculate acceptor levels relative to the conduction-band minimum, which varies more with supercell size than the top of the valence band does.

A correction to shallow-dopant levels in Si caused by the strain differences between different charge states of the impurity has been calculated by Rockett *et al.*[78] This correction is quite small in our calculations. For example, the levels of Ni_s shift by $\sim$0.03 eV, less than the typical error bar associated with the marker method.

VII. KEY POINTS AND DISCUSSION

The basic properties of interstitial Ti, Fe, and Ni and their interactions with the vacancy and the *A* center have been calculated using first-principles spin density-functional theory in Si_{216} periodic supercells and $3\times3\times3$ *k* point sampling (Si_{64} and $2\times2\times2$ for the NEB calculations). The gap levels have been estimated using our implementation of the marker method, which uses the perfect crystal used as a universal marker.

For the isolated interstitials, the equilibrium site, spin state, gap levels, and activation energies for diffusion are in very good agreement with the available experimental data for Ti_i, Fe_i, and Cu_i. In the case of Ni_i, we predict it to be 0.21 eV, less than half the most commonly quoted value in the literature. However, there is no agreement in the literature on the diffusivity of Ni_i.[63]

The donor and the acceptor levels of Ni_i are predicted to be just below the top of the valence band and just above the bottom of the conduction band, respectively. Therefore, Ni_i is in the 0 charge state for all positions of the Fermi level.

TM_i+V forms TM_s with an energy gain ranging from 2.7 to 3.2 eV, which is less than the formation energy of the vacancy, 3.96 eV. Therefore, vacancies must be provided in order for the reaction to take place. The electrical properties of the TM_s's are opposite of those of the TM_i's. Ti_i has a double donor and donor level as well as an acceptor level in the gap while Ti_s has only shallow donor and acceptor levels. Fe_i has a deep donor while Fe_s has a deep acceptor level. Ni_i is always in the 0 charge state while Ni_s has deep donor, acceptor, and double acceptor levels in the gap. Thus, if Ti_i traps a vacancy, it is almost passivated while in *p*-Si, the donor level of Fe_i is passivated, but a deep-acceptor level appears. This level is not expected to be a significant trap for minority carriers in *p*-Si.

The strong interactions between TM_i's and vacancies result in substantial changes in the electrical activity of the TM. This suggests that vacancies may be playing an unrecognized role during a variety of nonequilibrium processes that generate them. In general, most of the attention paid to 3*d* TM impurities focuses on the isolated interstitial or on a few well-known defects such as Fe-acceptor pairs. For example, the "Fe content" of *p*-Si samples is often obtained

from the amplitude of the DLTS lines of Fe_i and the $\{Fe_iB_s\}$ pair. In other words, it refers to the Fe_i content, not the total Fe. However, some of the TM impurities present in the melt could easily trap as isolated TM_s impurities and remain hidden from such DLTS analysis. More importantly, a number of processing steps are known (or believed) to inject vacancies into the bulk. These include implantation and irradiation of course, but also plasma exposure and a number of surface treatments (SiN_x antireflection coatings and Al back contacts in PV manufacturing), high temperature anneals and various types of rapid-thermal processing. How many vacancies are actually generated is not known and probably depends on the details of the process (anneal time, temperature ramps, densities of the surface layers, etc.). However, the generated vacancies diffuse rapidly and may well passivate some of the undesirable TM_i still present in the sample. The observed reduction in the DLTS amplitudes of the unwanted TM_i's is often attributed to gettering without direct evidence of how much gettering actually took place. Our results suggest that TM_s's will form, thus resulting in a reduction in the DLTS amplitudes and increase minority-carrier lifetimes. The (partial) passivation by vacancies (instead of H), first discussed in conjunction with Fe_i,[39] appears to extend to Ti_i as well. Further experimental studies of V production and TM_i+V interactions would clarify these issues.

The interactions between a TM_i and the $\{OV\}$ pair lead to the formation of two (almost) energetically degenerate complexes, $\{TM_i,O,V\}$ and $\{TM_s,O_i\}$. The former has the TM_i just outside the A center and the latter consist of a TM_s with O_i bridging an adjacent Si-Si bond. The acceptor level of the "{FeVO}" defect reported by several authors[28,76,77] matches more closely that of $\{Fe_i,O,V\}$ than of $\{Fe_s,O_i\}$.

ACKNOWLEDGMENTS

This work is supported in part by the Grant No. D-1126 from the R.A. Welch Foundation and by the Silicon Solar Consortium. S.K.E. acknowledges useful discussions with T. Buonassisi, who also pointed out the qualitative connection to the work of L. Pauling. Many thanks to Texas Tech's High Performance Computer Center for generous amounts of computer time.

*stefan.estreicher@ttu.edu

[1] J. D. Struthers, J. Appl. Phys. **27**, 1560 (1956).
[2] C. B. Collins and R. O. Carlson, Phys. Rev. **108**, 1409 (1957).
[3] E. R. Weber, Appl. Phys. A: Solids Surf. **30**, 1 (1983).
[4] A. A. Istratov and E. R. Weber, Appl. Phys. A: Mater. Sci. Process. **66**, 123 (1998).
[5] A. A. Istratov, H. Hieslmair, and E. R. Weber, Appl. Phys. A: Mater. Sci. Process. **69**, 13 (1999).
[6] A. A. Istratov, H. Hieslmair, and E. R. Weber, Appl. Phys. A: Mater. Sci. Process. **70**, 489 (2000).
[7] A. A. Istratov, T. Buonassisi, M. Heuer, M. Pickett, and E. R. Weber, in *Proceedings of the 15th Workshop on c-Si Solar Cells and Modules: Materials and Processes*, edited by B. L. Sopori (NREL, Golden, CO, 2005), pp. 70–77.
[8] A. Rohatgi, J. R. Davis, R. H. Hopkins, P. Rai-Choudhury, P. G. McMullin, and J. R. McCormick, Solid-State Electron. **23**, 415 (1980).
[9] J. T. Borenstein, J. I. Hanoka, B. R. Bathey, J. P. Kalejs, and S. Mil'shtein, Appl. Phys. Lett. **62**, 1615 (1993).
[10] R. Davis, Jr., A. Rohatgi, R. H. Hopkins, P. D. Blais, P. Rai-Choudhury, J. R. McCormick, and H. C. Mollenkopf, IEEE Trans. Electron Devices **27**, 677 (1980).
[11] H. H. Woodbury and G. W. Ludwig, Phys. Rev. **117**, 102 (1960).
[12] G. W. Ludwig and H. H. Woodbury, Phys. Rev. Lett. **5**, 98 (1960).
[13] G. W. Ludwig and H. H. Woodbury, Solid State Phys. **13**, 223 (1962).
[14] L. A. Hemstreet, Phys. Rev. B **15**, 834 (1977).
[15] G. G. DeLeo, G. D. Watkins, and W. B. Fowler, Phys. Rev. B **23**, 1851 (1981); **25**, 4962 (1982); **25**, 4972 (1982).
[16] A. Zunger and U. Lindefelt, Phys. Rev. B **26**, 5989 (1982).
[17] A. Zunger and U. Lindefelt, Phys. Rev. B **27**, 1191 (1983).
[18] H. Katayama-Yoshida and A. Zunger, Phys. Rev. B **31**, 8317 (1985).
[19] F. Beeler, O. K. Andersen, and M. Scheffler, Phys. Rev. Lett. **55**, 1498 (1985).
[20] J. Utzig, J. Appl. Phys. **65**, 3868 (1989).
[21] D. E. Woon, D. S. Marynick, and S. K. Estreicher, Phys. Rev. B **45**, 13383 (1992).
[22] S. Hocine and D. Mathiot, Appl. Phys. Lett. **53**, 1269 (1988).
[23] A. A. Istratov, C. Flink, H. Hieslmair, E. R. Weber, and T. Heiser, Phys. Rev. Lett. **81**, 1243 (1998).
[24] S. K. Estreicher, D. West, J. Goss, S. Knack, and J. Weber, Phys. Rev. Lett. **90**, 035504 (2003). Although this paper correctly describes the $\{Cu_iCu_s\}$ pair, it incorrectly assigns it to the "^{0}Cu" defect, which is now known to contain four Cu atoms; see M. Steger, A. Yang, N. Stavrias, M. L. W. Thewalt, H. Riemann, N. V. Abrosimov, M. F. Churbanov, A. V. Gusev, A. D. Bulanov, I. D. Kovalev, A. K. Kaliteevskii, O. N. Godisov, P. Becker, and H.-J. Pohl, *ibid.* **100**, 177402 (2008).
[25] A. C. Wang and C. T. Sah, J. Appl. Phys. **56**, 1021 (1984).
[26] K. Graff, *Metal Impurities in Silicon-Device Fabrication* (Springer, Berlin, 1995).
[27] P. Kaminski, R. Kozlowski, A. Jelenski, T. Mchedlidze, and M. Suezawa, Jpn. J. Appl. Phys., Part 1 **42**, 5415 (2003).
[28] B. A. Komarov, Fiz. Tekh. Poluprovodn. **38**, 1079 (2004) [Semiconductors **38**, 1041 (2004)].
[29] S. H. Müller, G. M. Tuynman, E. G. Sieverts, and C. A. J. Ammerlaan, Phys. Rev. B **25**, 25 (1982).
[30] V. P. Markevich, A. R. Peaker, I. F. Medvedeva, V. E. Gusakov, L. I. Murin, and B. G. Svensson, Solid State Phenom. **131-133**, 363 (2008).
[31] V. P. Markevich, A. R. Peaker, I. F. Medvedeva, V. E. Gusakov, L. I. Murin, and B. G. Svensson, ECS Trans. **18**, 1013 (2009).
[32] B. G. Svensson, M. O. Aboelfotoh, and J. L. Lindström, Phys. Rev. Lett. **66**, 3028 (1991).
[33] M. O. Aboelfotoh and B. G. Svensson, Phys. Rev. B **52**, 2522 (1995).

[34] W. Jost and J. Weber, Phys. Rev. B **54**, R11038 (1996).
[35] M. Shiraishi, J.-U. Sachse, H. Lemke, and J. Weber, Mater. Sci. Eng., B **58**, 130 (1999).
[36] W. Jost, J. Weber, and H. Lemke, Semicond. Sci. Technol. **11**, 22 (1996); **11**, 525 (1996).
[37] S. Knack, J. Weber, H. Lemke, and H. Riemann, Phys. Rev. B **65**, 165203 (2002).
[38] D. J. Backlund and S. K. Estreicher, in *Defects in Inorganic Photovoltaic Materials*, MRS Symposia Proceedings Vol. 1268, edited by D. Friedman, M. Stavola, W. Walukiewicz, and S. Zhang (Material Research Society, Warrendale, PA, 2010).
[39] S. K. Estreicher, M. Sanati, and N. Gonzalez Szwacki, Phys. Rev. B **77**, 125214 (2008).
[40] M. Sanati, N. Gonzalez Szwacki, and S. K. Estreicher, Phys. Rev. B **76**, 125204 (2007).
[41] S. K. Estreicher, D. West, and P. Ordejón, Solid State Phenom. **82-84**, 341 (2002).
[42] D. West, S. K. Estreicher, S. Knack, and J. Weber, Phys. Rev. B **68**, 035210 (2003).
[43] S. K. Estreicher, Phys. Rev. B **60**, 5375 (1999).
[44] *Theory of Defects in Semiconductors*, edited by D. A. Drabold and S. K. Estreicher (Springer, Berlin, 2007).
[45] D. Sánchez-Portal, P. Ordejón, E. Artacho, and J. M. Soler, Int. J. Quantum Chem. **65**, 453 (1997).
[46] E. Artacho, D. Sánchez-Portal, P. Ordejón, A. García, and J. M. Soler, Phys. Status Solidi B **215**, 809 (1999).
[47] H. J. Monkhorst and J. D. Pack, Phys. Rev. B **13**, 5188 (1976).
[48] A. Resende, R. Jones, S. Öberg, and P. R. Briddon, Phys. Rev. Lett. **82**, 2111 (1999).
[49] J. P. Goss, M. J. Shaw, and P. R. Briddon, *Theory of Defects in Semiconductors* (Ref. 44), p. 69.
[50] G. Mills and H. Jonsson, Phys. Rev. Lett. **72**, 1124 (1994); H. Jonsson, G. Mills, and K. W. Jacobsen, in *Classical and Quantum Dynamics in Condensed Phase Simulations*, edited by B. J. Berne, G. Ciccotti, and D. F. Coker (World Scientific, Singapore, 1998), p. 385.
[51] G. Henkelman, B. P. Uberuaga, and H. Jonsson, J. Chem. Phys. **113**, 9901 (2000); G. Henkelman and H. Jonsson, *ibid.* **113**, 9978 (2000).
[52] N. Troullier and J. L. Martins, Phys. Rev. B **43**, 1993 (1991).
[53] L. Kleinman and D. M. Bylander, Phys. Rev. Lett. **48**, 1425 (1982).
[54] V. L. Moruzzi and C. B. Sommers, *Calculated Electronic Properties of Ordered Alloys: A Handbook* (World Scientific, Singapore, 1995).
[55] J. M. Pruneda, R. Robles, S. Bouarab, J. Ferrer, and A. Vega, Phys. Rev. B **65**, 024440 (2001).
[56] J. P. Perdew, K. Burke, and M. Ernzerhof, Phys. Rev. Lett. **77**, 3865 (1996).
[57] O. F. Sankey and D. J. Niklewski, Phys. Rev. B **40**, 3979 (1989); O. F. Sankey, D. J. Niklewski, D. A. Drabold, and J. D. Dow, *ibid.* **41**, 12750 (1990).
[58] D. West and S. K. Estreicher, Phys. Rev. Lett. **96**, 115504 (2006); Phys. Rev. B **75**, 075206 (2007).
[59] D. A. van Wezep and C. A. J. Ammerlaan, J. Electron. Mater. **14a**, 863 (1985).
[60] D. A. van Wezep, R. van Kemp, E. G. Sieverts, and C. A. J. Ammerlaan, Phys. Rev. B **32**, 7129 (1985).
[61] D. A. van Wezep and C. A. J. Ammerlaan, Phys. Rev. B **37**, 7268 (1988).
[62] M. K. Bakhadyrkhanov, S. Zainabidinov, and A. Khamidov, Fiz. Tekh. Poluprovodn. **14**, 412 (1980) [Sov. Phys. Semicond. **14**, 243 (1980)].
[63] F. H. M. Spit, D. Gupta, and K. N. Tu, Phys. Rev. B **39**, 1255 (1989).
[64] G. D. Watkins, in *Handbook of Semiconductor Technology, Electronic Structure and Properties of Semiconductors*, edited by K. A. Jackson and W. Schröter (Wiley-VCH, Weinheim, 2000), Vol. 1, Chap. 3.
[65] L. Pauling, Phys. Rev. **54**, 899 (1938).
[66] H. Kitagawa and H. Nakashima, Phys. Status Solidi A **99**, K49 (1987).
[67] A. A. Istratov, C. Flink, H. Hieslmair, T. Heiser, and E. R. Weber, Appl. Phys. Lett. **71**, 2121 (1997).
[68] M. Seibt, H. Hedemann, A. A. Istratov, F. Riedel, A. Sattler, and W. Schröter, Phys. Status Solidi A **171**, 301 (1999).
[69] N. T. Son, T. Gregorkiewicz, and C. A. J. Ammerlaan, Phys. Rev. Lett. **69**, 3185 (1992).
[70] N. T. Son, A. B. van Oosten, and C. A. J. Ammerlaan, Solid State Commun. **80**, 439 (1991).
[71] L. S. Vlasenko, N. T. Son, A. B. van Oosten, C. A. J. Ammerlaan, A. A. Lebedev, E. S. Taptygov, and V. A. Khramtsov, Solid State Commun. **73**, 393 (1990).
[72] B. Effey-Schwickert, M. Wiegand, H. Vollmer, and R. Labusch, Appl. Phys. A: Mater. Sci. Process. **77**, 711 (2003).
[73] G. D. Watkins and P. M. Williams, Phys. Rev. B **52**, 16575 (1995).
[74] C. A. J. Ammerlaan and A. B. van Oosten, Phys. Scr. **T25**, 342 (1989).
[75] B. Pajot, in *Oxygen in Silicon*, Semiconductor and Semimetals Vol. 42, edited by F. Shimura (Academic, San Diego, 1994), p. 191.
[76] C. E. Barnes, J. Electron. Mater. **8**, 437 (1979).
[77] Z. You, M. Gong, Y. Chen, and J. W. Corbett, J. Appl. Phys. **63**, 324 (1988).
[78] A. Rockett, D. D. Johnson, S. V. Khare, and B. R. Tuttle, Phys. Rev. B **68**, 233208 (2003).